ELSEVIER

Thermochimica Acta 321 (1998) 161–165

thermochimica acta

Characterization of ancient magnesian mortars coming from northern Italy

S. Bruni[a,*], F. Cariati[a], P. Fermo[a], A. Pozzi[a], L. Toniolo[b]

[a] *Dipartimento di Chimica Inorganica Metallorganica e Analitica, Università di Milano, Via G. Venezian 21, 20133 Milan, Italy*
[b] *Centro C.N.R. "Gino Bozza" per lo studio delle cause di deperimento e dei metodi di conservazione delle opere d'arte, P.za L. da Vinci 32, 20133 Milan, Italy*

Received 25 February 1997; accepted 24 April 1998

Abstract

Different ancient mortar samples were analyzed to characterize their binder fraction. Thermal analyses (TG, DSC) proved to be very useful in the identification of three different species of lime composed of: (a) only calcite; (b) calcite and magnesite; (c) calcite, hydromagnesite and magnesite. The hydromagnesite is well identified in the DSC curve showing the peaks corresponding to the three-step thermal decomposition. Also the same mineral was detected by FTIR and/or micro-FTIR analyses, depending on its amount in the binder fraction of the mortar. Actually, the two absorption peaks characteristic of the hydromagnesite were often hidden by the wider peaks due to the asymmetric stretching of the carbonate ion, observed for the calcite and magnesite. © 1998 Elsevier Science B.V.

Keywords: Ancient mortars; Hydromagnesite; IR spectroscopy; Thermal analyses

1. Introduction

Studies about historical mortars containing magnesian lime have already been published by Chiari et al. [1], Newton and Sharp [2] and Vecchio et al. [3]. A series of mortar samples coming from different monuments of northern Italy was investigated by the X-ray powder diffraction technique, and the presence of magnesite together with hydromagnesite was confirmed [4]. Some of these samples were further examined with the aim of demonstrating that the presence of calcite, hydromagnesite and magnesite could be revealed by thermogravimetric and FT-IR analyses, indicating precisely the compositional features of the binder fraction. The samples were chosen from among a large number of mortars analyzed during recent years, both for their high and different contents of magnesium (i.e. for the different raw materials employed in their preparation) and for their different functions (i.e. for the differences in the binder-aggregate mixture).

2. Experimental

2.1. Sampling

Table 1 presents information regarding the function, age and provenance of the mortar samples. The samples were collected during the conservation works of different monuments to carry out the analytical investigations.

*Corresponding author. Tel.: +39 2 23993930; fax: +39 2 70602899; e-mail: toniolo@cdc8g5.cdc.polimi.it

PII: S0040-6031(98)00455-9

Table 1
Description of the ancient mortar samples

Sample	Function	Age (century)	Location
1	painted plaster	XV	Frescoes by V. Foppa, Church of S. Eustorgio – Milan
2	outside plaster covering the masonry	VI–VII	Church of S. Fedelino – Novate Mezzola, Sondrio
3	outside plaster covering the masonry	XVII	Sanctuary of the Beata Vergine – Grosotto, Sondrio
4	outside plaster covering the masonry	XV	Church of S. Maria presso S. Satiro – Milan
5	bedding mortar for brick masonry	XV	Church of S. Maria Incoronata – Lodi

The considered samples were chosen for the characteristics of the binder fraction containing different amount of magnesium. The differences in the provenance and age were intentionally ignored because the goal of the work was to assess the potential of the applied analytical techniques.

2.2. Instrumental methods

Thermogravimetric analyses were performed by a Perkin–Elmer TGA 7 analyzer in a nitrogen atmosphere at a heating rate of $10^{\circ}C\ min^{-1}$. The instrument has been calibrated using a standard calibration procedure which enables to perform Curie-point calibrations with two calibrating standards (a nickel and an iron standard were used). Derivative curves of the scans (DTG) were employed to determine the decomposition temperatures.

Differential scanning calorimetry (DSC) curves were obtained by a Perkin-Elmer DSC 7 instrument under a nitrogen atmosphere at a heating rate of $10^{\circ}C\ min^{-1}$ with reference to the melting temperatures of two standards, namely those of indium and zinc. Powdered samples were placed in Al pans with pin-holed lids.

ICP emission atomic spectra were recorded, by a Jobin–Yvon JY 24 spectrophotometer, on solutions obtained by treating the residuals of TG analysis with 3 ml of 37% w/v hydrochloric acid and then diluting to 10 ml with milli-Q water.

FTIR transmission spectra in the 4000–400 cm^{-1} range were carried out using a Digilab FTS-40 spectrophotometer on KBr pellets of powdered samples.

Micro-FTIR specular reflectance spectra were collected in the 4000–700 cm^{-1} range on polished cross sections of the mortars, using a Jasco WS-IR 100 spectrophotometer equipped with an MCT detector. Sample areas of ca. 1000 μm^2 were examined and the reflectance spectra were converted by the Kramers–Kronig transform into transmittance spectra.

3. Results and discussion

3.1. ICP analyses

All the examined mortar samples, except those coming from S. Maria Incoronata (Sample 5 in Table 1), showed the presence of both calcium and magnesium. The obtained Ca/Mg weight percentage mean ratios were as follows: 3.57 (Sample 1), 2.43 (Sample 2), 11.88 (Sample 3) and 1.90 (Sample 4), indicating that the magnesium content was different according to the lime binder used. In the case of Sample 5, the binder fraction was constituted of calcitic lime.

3.2. Thermal analyses

The methods of thermal analysis, TGA and DSC, proved to be very useful in identifying the three carbonate phases contained in the mortar samples.

Fig. 1(a–c) shows the TG curves of the powders obtained from samples 3, 4 and 5 containing, respectively, calcite, magnesite and hydromagnesite, only calcite and magnesite, only calcite. The mineralogical composition of these samples was known after XRD powder diffraction [4].

The derivative curve (DTG) of the scan of Sample 3 exhibited four peaks, corresponding to the four inflections observed in Fig. 1(c) at ca. 230°, 380°, 430° and 650°C. Two peaks are observed in the DTG curve of Sample 4, at ca. 450° and 670°C. Finally, only one peak appeared for Sample 5 at ca. 670°C. This obviously corresponded to the decomposition of

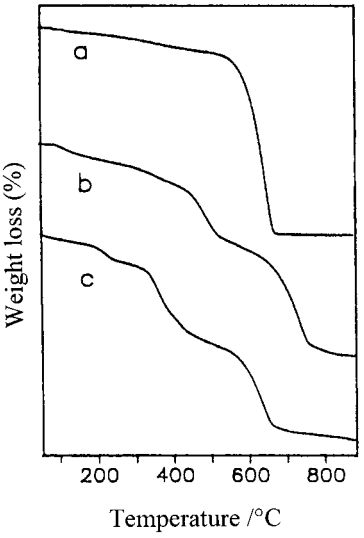

Fig. 1. TG curves of binder powders from: (a) bedding mortar for brick masonry (Church of S. Maria Incoronata, Lodi); (b) outside plaster covering the masonry (Church of S. Maria presso S. Satiro, Milano); (c) outside plaster covering the masonry (Santuario of the Beata Vergine, Grosotto, Sondrio).

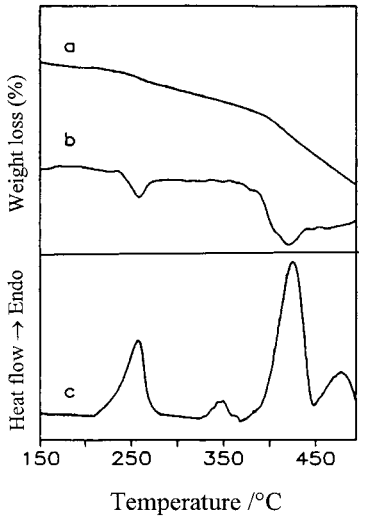

Fig. 2. (a) TG, (b) DTG and (c) DSC curves for outside plaster covering the masonry (Church of S. Fedelino, Novate Mezzola, Sondrio).

calcite:

$$CaCO_3 \rightarrow CaO + CO_2 \quad (1)$$

As a consequence, the low-temperature peak observed for Sample 4 could be assigned to the decomposition of magnesite:

$$MgCO_3 \rightarrow MgO + CO_2 \quad (2)$$

Finally, on this basis, it was hypothesized that the two peaks at 230° and 380°C that appeared in the DTG curve for Sample 3 could be assigned, respectively, to the loss of crystallization water and to the decomposition of hydromagnesite carbonate [3].

As the thermal decomposition of hydromagnesite also includes the loss of hydroxyl water, the process can be described as follows:

$$4MgCO_3 \cdot Mg(OH)_2 \cdot 4H_2O \rightarrow 4MgCO_3 \cdot Mg(OH)_2 + 4H_2O \quad (3)$$

$$4MgCO_3 \cdot Mg(OH)_2 \rightarrow 4MgCO_3 + MgO + H_2O \quad (4)$$

$$MgCO_3 \rightarrow MgO + CO_2 \quad (5)$$

DSC analysis proved to be very useful in determining the temperature range for the samples, where this process took place. In Fig. 2, it is possible to compare the TG, DTG and DSC curves of Sample 2, that was characterized by a composition similar to that of Sample 3 (the temperature range considered in the figure does not include the decomposition of calcite). The DSC curve (Fig. 2(c)) showed four endothermic peaks at 250°, 350°, 410° and 480°C, but only the 250°, 410° and 480°C peaks corresponded perfectly to those observed in the DTG curve (Fig. 2(b)). They should be assigned, respectively, to the dehydration of hydromagnesite, to the decomposition of hydromagnesite carbonate and that of magnesite. It should be remarked that, for Sample 2, these processes took place at rather different temperatures as compared with those observed for the same decomposition in Sample 3. This is not surprising, as the effective decomposition temperatures depend on various factors, including the degree of crystallinity and the particle size of the powder sample. Therefore, for each process, only a temperature range can be defined and the whole pattern of the scan is more meaningful for its interpretation than the single peak temperatures of the DTG curves. In the DSC curve (Fig. 2(c)), a fourth peak was observed at 350°C, and that could be assigned to the loss of hydroxyl water in hydromagnesite, expressed in Eq. (4)[5]. In the corresponding DTG curve (Fig. 2(b)) no peak was detected at that

temperature, probably because it is hindered by the adjacent peak corresponding to the decomposition of carbonate of hydromagnesite.

The above assignments were confirmed by comparing the weight losses measured for the corresponding processes in the TG curves with the relative amounts of calcium and magnesium contained in the residuals of thermogravimetric analysis and determined by ICP emission atomic spectroscopy. For all mortars listed in Table 1, a good agreement was obtained between the determined calcium and magnesium contents and the weight losses due to thermal decomposition.

Finally, it is noteworthy that, at temperatures <200°C, the scans of the examined samples exhibited a 2–5% weight loss, attributable to the hydration water of the silicates constituting the aggregate of mortars.

It should be noted that the above interpretation of the thermal behavior of the examined mortar samples is consistent with the results obtained by Chiari et al. [1], Newton and Sharp [2] and Vecchio et al. [3]. However, while Newton and Sharp did not observe, or recognize, the presence of hydromagnesite in their samples, Chiari et al. assumed that, in mortars, usually magnesium hydroxide transforms only in the basic carbonate. On the contrary, on the basis of the reported thermal analysis and in accordance with Vecchio et al. [3], the presence of both magnesite and hydromagnesite was assessed for the considered samples.

3.3. IR spectroscopy

The IR spectra of calcite and magnesite exhibited, for the asymmetric stretching of the carbonate ion, a single broad band, respectively, in the 1435–1410 and 1478–1450 cm^{-1} frequency ranges. [6,7]. On the contrary, for hydromagnesite two bands were observed, at ca. 1420 and 1480 cm^{-1} [8,9], indicating site distortion and the presence of two distinct kinds of carbonate ions in the crystal [10,11]. This peculiarity allows the recognition of the presence of hydromagnesite in the samples. The correspondence between the modifications of the IR spectra after the thermal treatment of the samples and the above interpretation of the thermal analyses was checked. For instance, the IR transmission spectrum of the binder fraction of Sample 2 (mechanically separated from the mortar) shows initially the characteristic bands of hydromagnesite (Fig. 3(a)), beyond the other carbonate phases (calcite and magnesite). After thermal treatment at 450°C, a single band was observed due to the carbonate ion of calcite and magnesite (Fig. 3(b)). After a further treatment at 580°C, this band appeared to be narrower and shifted to lower frequencies (Fig. 3(c)). This effect may be ascribed to the difference between the CO_3^{2-} stretching frequencies in calcite and magnesite (see above). A similar effect was observed in the spectra of Sample 4 while Sample 5, containing only calcite, did not show any spectral difference before and after heating.

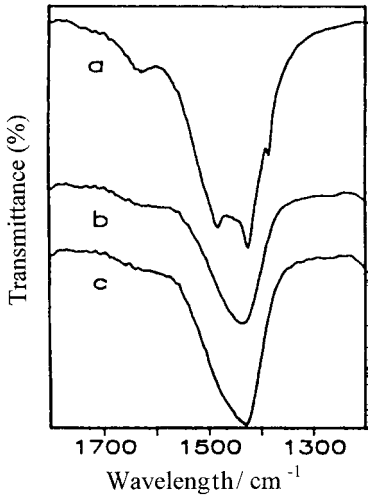

Fig. 3. FTIR transmission spectra of binder fraction from outside plaster covering the masonry (Church of S. Fedelino, Novate Mezzola, Sondrio): untreated sample (a); sample after thermal treatment at 450° (b) and 580°C (c).

By using micro-FTIR spectroscopy, it was possible to analyze selectively the binder fraction of the mortar samples. For those containing all three carbonate species, areas could be identified, where a significant amount of hydromagnesite was present (see, e.g. the transformed reflection spectrum of a suitable area of Sample 2, Fig. 4). On the contrary, micro FTIR spectra did not allow areas with a prevalence of magnesite to be distinguished from areas mainly constituted of calcite.

In summary, IR spectroscopy has proved to be an useful tool to detect the presence of hydromagnesite in mortar samples, even if it should be observed that, for very small amounts of this component, the corresponding bands could be too weak to be observed.

Fig. 4. FTIR transmission spectrum calculated from the specular reflection spectrum of a binder area (ca. 1000 μm^2) of a polished cross section of outside plaster covering the masonry (Church of S. Fedelino, Novate Mezzola, Sondrio).

4. Conclusions

The experimental data show that the analytical characterization of the binder fraction of mortar samples could be performed with the aid of IR spectroscopy and thermal analyses, together with the quantitative results obtained by ICP. These techniques allow the different carbonate species, that play the binder role in the mortar mixture, to be identified, employing a very small amount of sample (which is a very important requirement in the analysis of ancient mortars).

The combined results obtained for the considered mortars, allowed three different kinds of binder fraction to be distinguished, namely (a) calcitic lime containing only calcite, (b) magnesian lime composed of calcite and magnesite, and (c) magnesian lime composed of calcite, magnesite and hydromagnesite.

Finally, the natural process of carbonation of the lime containing brucite ($Mg(OH)_2$) leads, most frequently, to the formation of hydromagnesite as a stable phase together with magnesite.

References

[1] G. Chiari, M.L. Santarelli, G. Torraca, Materiali e Strutture 3 (1992) 111.
[2] R.G. Newton, J.H. Sharp, Studies in Conser. 32 (1987) 163.
[3] S. Vecchio, A. La Ginestra, A. Frezza, C. Ferragina, Thermochim. Acta 227 (1993) 215.
[4] S. Bruni, F. Cariati, P. Fermo, P. Cairati, G. Alessandrini, L. Toniolo, Archeometry 39 (1997) 1.
[5] W. Beck, Am. Mineralogist 35 (1950) 985.
[6] V.C. Farmer, The Infrared Spectra of Minerals, Mineralogical Society, London, 1974, p. 239.
[7] J.A. Gadsden, Infrared Spectra of Minerals and Related Inorganic Compounds, Butterworths, London, 1977, p. 62.
[8] T. Pobeguin, Compt. Rend. 248 (1959) 2220.
[9] J. Bessiere-Morandat, V. Lorenzelli, J. Lecomte, J. Physique 31 (1970) 309.
[10] M. Akao, F. Marumo, S. Iwai, Acta Cryst. B30 (1974) 2670.
[11] W.B. White, Am. Mineralogist 56 (1971) 46.